Drainage Density and Controlling Factors in Cascade Range, Oregon, USA

Wei Luo[*a], Tomasz Stepinski[b], and Yi Qi[a]
[a]Department of Geography, Northern Illinois University, DeKalb, IL 60115, USA;
[b]Lunar and Planetary Institute, 3600 Bay Area Boulevard, Houston, TX 77058, USA.

ABSTRACT

This paper demonstrates a feasibility of automated drainage density mapping on regional scales and in high resolution, using remotely sensed elevation data. Such maps offer affordable means of surveying large regions for variability in spatially extended features, which themselves are difficult to sense remotely, but are expressed by the drainage density. We show that the proposed mapping method can be achieved by a combined utilization of two novel techniques: the curvature-based stream delineation algorithm, and the at-point assignment of drainage density values. In order to showcase our concept we have generated a map of drainage density for the study area in the Oregon Cascade Range. The map shows a sharp contrast in landscape dissection. A number of factors, potentially responsible for that contrast, were considered, and the variation of the underlying geology was judged to be a major factor responsible for an observed drainage density pattern. Although the unique geological setting of the study area was know to us a priori, we envision applying our mapping method to locations where remotely sensed elevation is the only available data, and the generated map is used to extract new geologic or environmental information.

Keywords: Drainage density, Controlling factors, DEM, stream extraction

1. INTRODUCTION

Landscapes are observed to be dissected by intricate network of channels transporting rainwater to progressively lower elevations. Despite their fractal appearance these drainage networks do not extend to arbitrarily small scales, instead there exists a fundamental horizontal length scale, L_o, associated with dissection of a particular landscape. On scales $L < L_o$, rainwater flows overland without dissecting the surface. Thus, the value of L_o separates two very different physical regimes and its determination is important from theoretical, as well as practical, points of view [1-5]. Quantitative descriptors of drainage networks, such as stream or link frequency, mean link length, hillslope length, and texture have been developed [6] in order to assess the value of L_o, but perhaps the most broadly used method of assessing L_o is through calculation of drainage density.

Drainage density, D, has been defined [7] as the total length of stream channels L_T divided by the total area A; $D = L_T / A$. The fundamental length scale can be recovered from D as $L_o \approx 1/(2D)$ [7]. The original definition of D requires specification of area unit over which D is calculated; most frequently the entire study area or its constituent watershed basins are chosen as area units. In order to assure a high spatial resolution of D the study area must be subdivided into a large number of small (low order) basins. In many cases such division is impractical due to excessive labor, and, consequently, D is calculated with a very coarse spatial resolution. This is unfortunate inasmuch as the value of D changes on a variety of scales due to a number of different factors, including climate [8, 9], vegetation [10], soil and rock properties [11, 12], and topographic relief and slope [13, 1, 3].

Another issue with calculating D is the location of streams themselves. Historically, streams were delineated from high resolution topographic maps supplemented by field work. In absence of any field information the streams are derived from crenulation of elevation contours. This method is time consuming and problematic in low relief regions. For some

[*] wluo@niu.edu; phone (815)753-6828; fax (815)753-6872

areas, including most of the United States, current topographic maps depict streams already derived by either the crenulation method, manual interpretation of aerial images, or field work. In such case stream lengths can be measured from "blue lines" indicating the streams. However, this method has been criticized for being inaccurate in mountainous areas [14, 3].

In the absence of topographic maps, or when studying large regions, the drainage network can be automatically extracted from a digital elevation model (DEM) constructed from remotely sensed data. DEM is a raster dataset where each cell is assigned an elevation value corresponding to its locations. Shuttle Radar Topography Mission (SRTM) altimetry data has being utilized to build a global DEM with the resolution of up to 30 meters/cell. Much higher resolution DEMs are constructed for local areas using the Light Detection and Ranging (LiDAR) measurements. Drainage networks can be automatically extracted from the DEM by a computer algorithm. Software packages such as ESRI's ArcGIS, Rivix's RiverTolls, or TauDEM all employ variants of the D8 algorithm [15] for quick identification of drainage networks and subsequent calculation of D. The D8 algorithm is based on the concept of local drainage directions; each cell in a DEM is assigned a drainage pointer to one of the eight neighboring cells in the direction of the steepest slope. These pointers define a tree-like drainage network that extends to an every cell in the DEM thus lacking any characteristic scale. To obtain a network with a scale L_o it is necessary to prune it using a channelization criterion, based on either physical or phenomenological reasoning [15-17, 2]. Pruning the D8 network using the flow accumulation criterion is the easiest and most widely used method to automatically delineate the streams. For example, it has been employed to obtain the HYDRO1k global dataset of streams (edc.usgs.gov/products/elevation/gtopo30/hydro/). However, it needs to be pointed out that so-extracted network may depart significantly from actual streams because a good channelization criterion is difficult to design. In particular, a criterion based on the flow accumulation threshold leads to a network that could be locally over-extracted or under-extracted, as the criterion forces an (approximately) uniform drainage density on a landscape with variable degree of dissection.

These shortcomings limit the applicability of widely available software packages to perform efficient, yet accurate, regional mapping of drainage density from remotely sensed data. Fortunately, new kind of drainage extraction algorithms have been developed in recent years that provides better accuracy than the D8 algorithm. They identify segments of the terrain with concave upward morphology. Such segments, identified by positive planar curvature, are the areas where flow accumulates, mostly constituent parts of the channels. The advantage of such algorithms is that they identify valleys (and thus streams) directly without any pruning, so no channelization criterion is necessary, and networks in terrains with spatially variable degree of dissection are accurately delineated. The technical challenge in the curvature based algorithms is the actual calculation of the curvature because landscapes, especially landscapes as given by the DEMs, have complicated and "noisy" surfaces. In order to obtain continuous streams, Tarboton and Ames [18] had developed an algorithm that combines a simple identification of concave upward cells [19] with the D8 algorithm. Most recently, Molloy and Stepinski [20] have developed an algorithm that calculates terrain curvature directly from its definition, but employs a series of image processing techniques to assure that only true valleys are delineated.

In this paper we demonstrate the importance of using an accurate drainage network extraction algorithm in mapping regions where dissection (encapsulated by the value of D) is expected to be spatially variable. We also argue that when working with remotely sensed data (DEM), mapping the degree of terrain dissection is better achieved by calculating the value of L_o directly from the DEM, instead of subdividing the site into basins and calculating D for each basin separately. Direct calculation of L_o for each cell in the raster enables redefinition of the notion of drainage density from a variable that is defined for a specific unit area to a variable that is defined at every cell $D = 1/(2 L_o)$ making possible a continuous (raster) mapping of drainage density [5]. A region in the Cascade Range, Oregon, USA is chosen to illustrate our ideas. Mapping D continuously over this region reveals existence of a sharp contrast in landscape dissection between western and eastern parts of the region. We investigate possible factors responsible for that contrast. The overall methodology presented in this paper constitutes a plausible framework for using the available remotely sensed data (in this case the topography) to identify changes in variables, such as geology, for which the data are difficult to gather remotely.

2. THE STUDY AREA AND DATA SOURCE

The study area, located in Cascade Range, Oregon, USA, is defined by the following latitude longitude coordinates: southwest corner: -122.75˚, 43.31˚; northeast corner: -121.31˚, 45.26˚, an area of roughly 117 km by 216 km (see Figure 1). We have chosen this study area because it encompasses the two major subprovinces [21, 22] of the Cascade Range in Oregon: Western Cascades (western part of the study area) and High Cascades (eastern part of the study area). The Western Cascades are dominated by deeply dissected, layered, basaltic and andesite lavas, and volcaniclastic flows of

Eocene to Pliocene (Tertiary) age [23]. The High Cascades form a broad volcanic platform and represent a much younger geological terrain, higher in elevation but lower in relief than the Western Cascades, reflecting recent constructional volcanism rather than erosional forms [23]. Rock type is dominated by low gradient basaltic and andesitic lava flows, cinders, pumice, and volcanic ash, mostly from shield volcanoes, cones, and vents of Quaternary age. The young age of the surficial deposits results in poor soil development. Surface and subsurface hydraulic conductivities in young volcanic deposits are exceptionally high due to highly porous and permeable volcanic layers [23]. The lateral contiguity of the two lithologically similar but geomorphically and age distinct geological terrains within a single study area provides a unique opportunity to examine our assertions made in Section 1. Figure 1 shows a 3D perspective view of the study area; the geomorphic contrast between the western and the eastern parts is clearly visible.

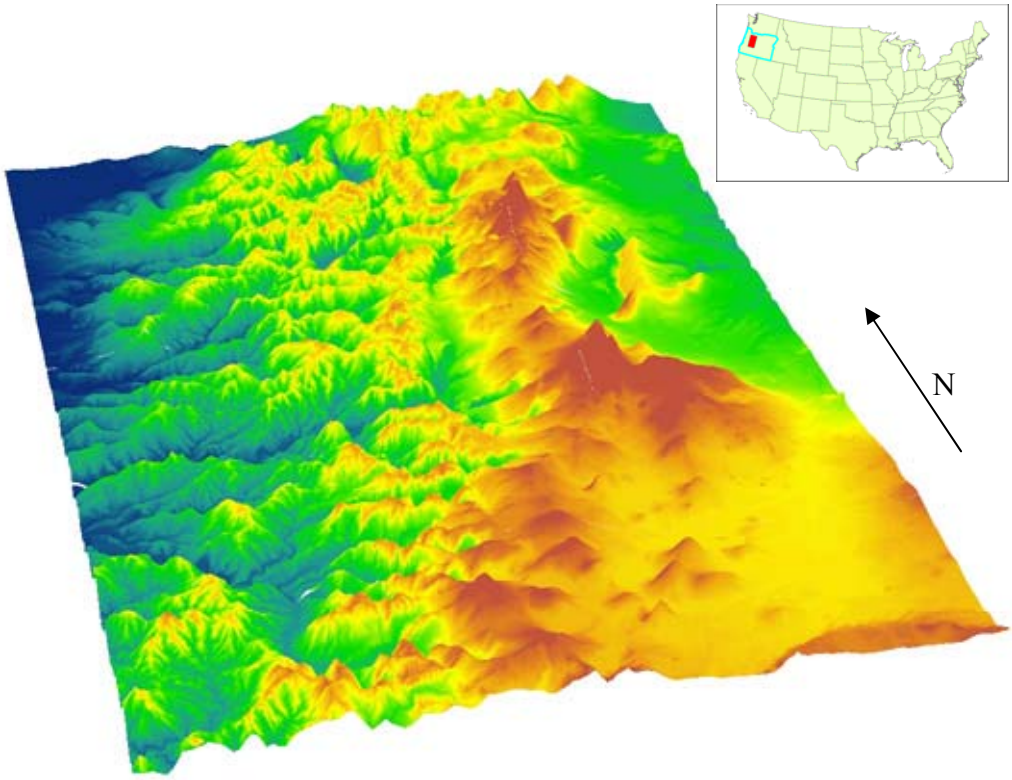

Fig. 1 3-D Perspective view of study area. Blue to orange color graduation shows low elevation to high elevation. The study area is roughly 117 km by 216 km (southwest corner: -122.75˚, 43.31˚; northeast corner: -121.31˚, 45.26˚)

The DEM data for the study area was downloaded from the National Elevation Dataset (NED) at http://seamless.usgs.gov/. The NED is a seamless mosaic of best-available elevation data. The resolution of the DEM is is 37.215 m. The precipitation data for the study area was extracted from the "United States Average Monthly or Annual Precipitation, 1971 – 2000" downloaded from PRISM website http://www.ocs.orst.edu/prism/products/. The geologic map was extracted from the digital version of Walker and MacLeod (1991) 1:500,000 scale Geologic Map of Oregon, downloaded at http://wrgis.wr.usgs.gov/docs/geologic/or/oregon.html.

3. METHOD AND RESULT

3.1 Extraction of streams from DEM

We view the DEM as "remotely sensed data" because in most cases the altimetry data, the raw ingredient of the DEM, is gathered remotely either by satellites or airborne instruments. In line with this reasoning, we consider extracting streams from the DEM as an automatic means of delineating drainage networks and, subsequently, the drainage density from

remotely sensed data. We believe that this is the only practical method to map drainage density on regional scale. Below, we report on extracting the streams using the popular D8 algorithm and the new, curvature-based algorithm.

3.1.1 Drainage directions (D8) based method

We have used the D8 algorithm as implemented in the ESRI's ArcGIS software package. The reference to the D8 algorithm is a shortcut because the algorithm itself is only one of many necessary to perform the task. The entire procedure involves the following steps. (1) To fill depressions in the DEM to make it fully drainable. This step is necessary because the DEM contains vertical errors that manifest themselves as spurious pits. (2) To compute drainage directions based on the steepest decent of each cell (the actual D8 algorithm). This results in a network of drainage directions extending to every cell in the raster. (3) To calculate flow accumulation based on drainage directions. The flow accumulation is the amount of rainwater that drains through a given point (cell) from all upward locations connected to that point by an uninterrupted chain of drainage directions. The flow accumulation, which cannot be calculated without knowing the rainfall rates, is represented by so-called contributing area, an upward area (in units of cells) that drains through a given point. (4) To prune the network of drainage directions using the threshold on the contribution area. The cells having contribution area smaller than a given critical value are pruned away. The rationale for such criteria is that channelization occurs only in places where there is significant enough flow. Figure 2(a) shows the streams extracted using this method with the contribution area threshold set to 300 cells. The value of the threshold was chosen so the density of streams in the western part of the study area is approximately equal to the density obtained using the curvature-based extraction method. The resultant network has approximately uniform density (an artifact of an oversimplified channelization criterion) contrary to what is reported in geologic assessments and what is visible in the 3-D rendition shown in Figure 1. In fact, the eastern, less dissected part of the region, appears slightly more dissect than the western part. Choosing a different threshold would change the density of the network but not its uniformity. Clearly, automatic extraction of stream via the D8 algorithm and the channelization criterion based on the contribution area leads to unacceptable results.

3.1.2 Curvature-based method

The biggest drawback of the drainage directions based method is the channelization criterion. The final distribution of streams is only as good as the pruning criterion. Criteria other than a threshold on contribution area have been investigated (see [18] for a review) but none is satisfactory. This is because a channelization criterion that is supposed to encapsulate the knowledge about physics of channelization is lacking. The curvature-based method avoids this difficulty by delineating channels directly from data without any reference to channelization mechanisms. It identifies channels as segments of terrain having concave upward (U-like shape) morphology. The method requires careful calculation of planar curvature. Positive values of planar curvature identify terrain with the concave upward morphology. It also requires reconnecting multiple identified segments into a continuous drainage network. We have mapped streams in the study area using the curvature-based algorithm recently developed by Molloy and Stepinski [20]. The procedure involves the following steps. (1) To compute topographic planar curvature. Available implementations, such as for example, in ESRI's ArcGIS, return noisy, unusable raster of curvature. We use a custom-made algorithm that smoothes the original surface and than fits a two-dimensional, second order polynomial to local patches of smoothed surface. The curvature is calculated analytically from the polynomial. (2) To threshold the curvature raster in order to identify locations characterized by positive curvature. In principle this threshold should be equal to 0 (identification of all positive values), however, channels are characterized by relatively large curvature, so threshold with a value of 0.003 is chosen. The result is a collection of disconnected terrain segments representing channels' fragments. (3) To connect the disconnected fragments using the drainage directions. The network of drainage directions is used as auxiliary information to aid the connection of various channels segments.

Interestingly, Molloy and Stepinski algorithm was originally developed to identify valley networks on planet Mars. Valley networks are geomorphic features reminiscent of terrestrial stream networks, but characterized by high spatial variability of dissection. It was subsequently applied [24] to map valley networks over large areas on Mars with high degree of accuracy. Figure 2(b) shows the streams within our study area extracted using the Molloy and Stepinski algorithm. The overall pattern of dissection is strikingly different from the uniform pattern produced by the D8-based algorithm (Figure 2(a)). The curvature-based method yields spatially variable degree of dissection, with the western part of the study area more densely dissected than its eastern part. This is in agreement with geologic assessments and visual evidence (see Figure 1).

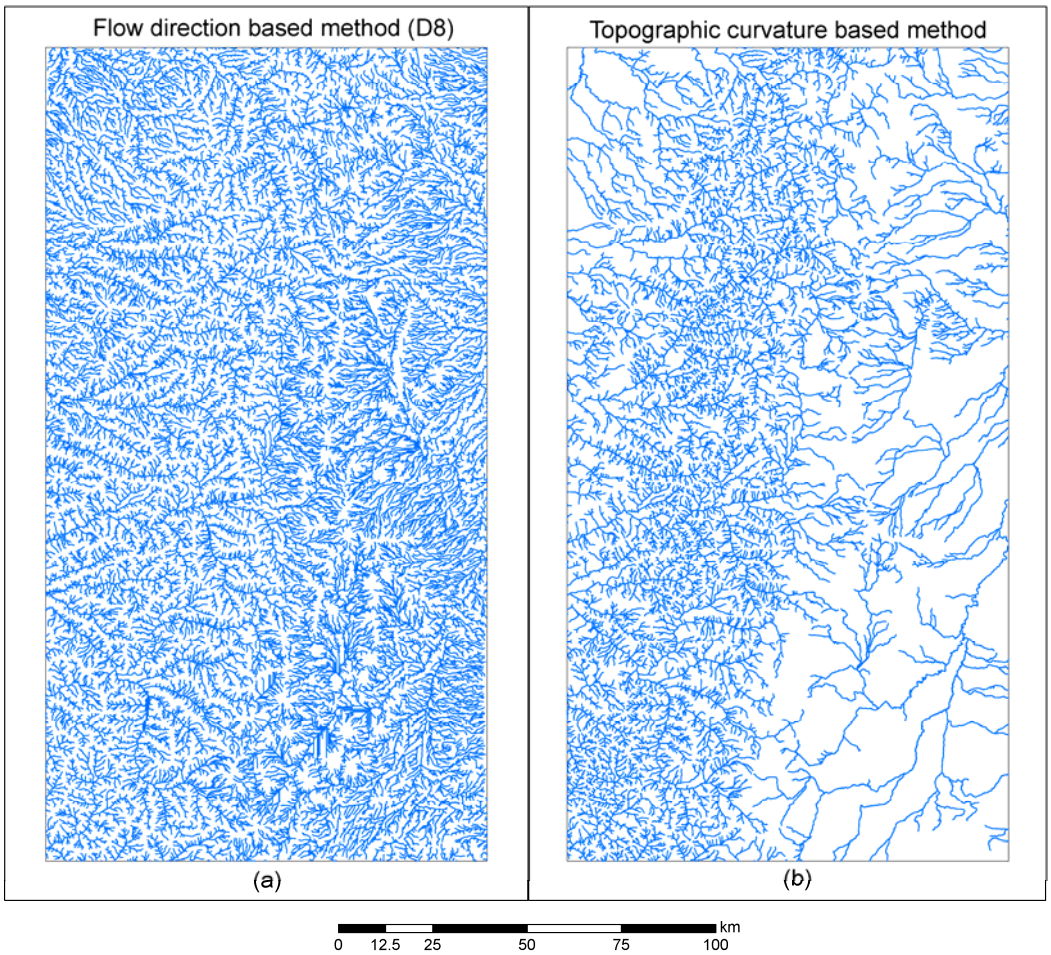

Fig. 2 Comparison of stream networks extracted from DEM using (a) flow direction based D8 method with 300 cells as flow accumulation threshold and (b) topographic curvature based method with 0.003 as the curvature threshold.

3.2 Drainage density calculation

Maps of stream networks (see Figure 2) can be used to visually assess the spatial variability of dissection. However, for quantitative analysis of factors controlling the variability of landscape dissection, a raster map encapsulating information present in stream networks is preferable. This goal is achieved by mapping the drainage density. Below we report on mapping the drainage density in the study area using the traditional definition of D with watershed basins as area units, as well as using the direct, at-point calculation of fundamental length scale L_o.

3.2.1 Mapping drainage density using watershed as area unit

As discussed in Section 1, a watershed basin is the area unit most commonly used in drainage density calculation. Given a drainage network (Figure 2), the drainage density is calculated by dividing the total length of the network in a given basin by the total area of that basin. We have divided the study area into watershed basins containing 4^{th} or higher Strahler order streams using ArcGIS, and calculated the drainage density for each basin separately using streams delineated by methods described in the previous section. Figure 3 shows maps of drainage density obtained using this procedure. Note that boundaries of watershed basins are fixed by the DEM, independent from extracted stream networks and thus identical on Figures 3(a) and 3(b). The maps of D reflect patterns of stream networks seen on Figure 2. Using streams delineated by the D8 algorithm results in the map of D that shows minimum spatial variability; the enhancement of D in the eastern part of the study area is consistent with what is seen on Figure 2(a). Using streams delineated by the curvature-based algorithm results in the map of D broadly in agreement with the network shown on Figure 2(b).

However, the contrast in the degree of dissection seen on Figure 2(b) appears sharper than what is seen on Figure 3(b). This is due to the course resolution of the drainage density map. The map is able to show variations on the length scale of an individual basin or larger, whereas an observed contrast occurs on a smaller scale. One solution would be to use smaller basins, however, a better solution is to calculate D at-point from the values of L_o, thus achieving the highest possible spatial resolution.

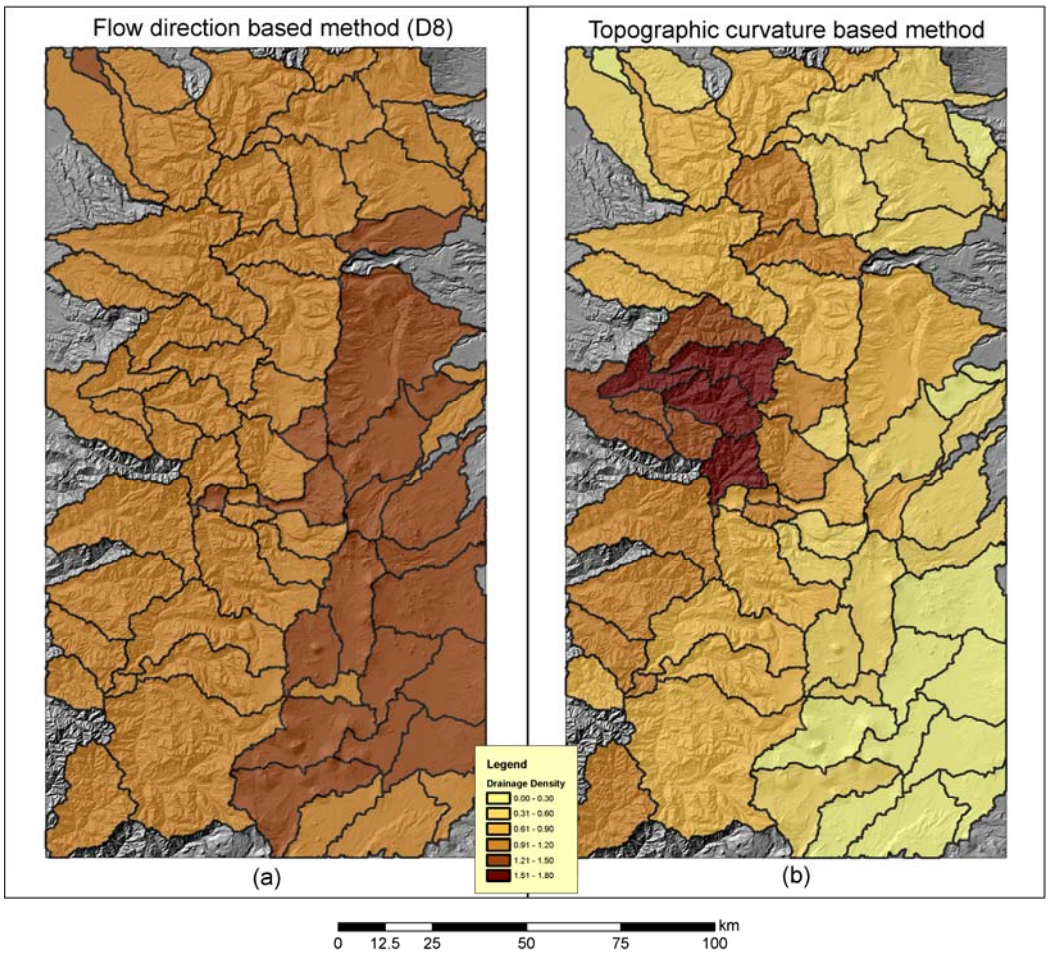

Fig. 3 Comparison of drainage density map for (a) D8 method and (b) curvature based method. Only 4th order or higher basins are shown. Shaded relief is shown in the background. The drainage density is calculated by using total stream length divided by area of watershed basin. The unit is km^{-1}. The same color gradation and division scheme is used for easy comparison.

3.2.2 Mapping drainage density using at-point values of dissection length scale

As we have noted in Section 1, drainage density and dissection length scale measure the same fundamental quantity – a degree of terrain dissection. In the absence of DEM data and fast computers calculating L_o directly was not feasible hence attention had focused on calculating drainage density. However, presently a direct, at-point calculation of L_o is feasible and can be used for at-point evaluation of D. Tucker et al. [5] have recently proposed a method of calculating drainage density based on exactly that principle. The basic idea is to calculate the local value of L_o from statistics of cell-to-stream length in the neighborhood of the focus cell. The cell-to-stream length, $L(x, y)$ is the downslope distance to the nearest stream from a given cell (x, y) following the path of steepest descent. This variable, which is defined for every cell in the raster, has a small value in places where stream network is dense and a large value in the places where the stream network is coarse. Of course, due to complicated morphology of landscape surfaces, two neighboring cells may have very different values of L because they may happen to be located at the two sides of the watershed boundary. This is why L itself is not a suitable measure of dissection, because the result would be noisy. Instead, Tucker et al. [5]

proposed defining L_o *(x,y)*= ⟨*L*⟩, where ⟨*L*⟩ is the mean value of *L* over a specified neighborhood of *(x, y)*. Such neighborhood should have a size equal to the autocorrelation length of *L(x,y)*. This is the longest length lag over which the values of *L(x,y)* are statistically related. The drainage density is given by $D = 1/(2 L_o)$ and is also defined at every cell in the raster.

We have applied Tucker et al. method of calculating *D* to our study area using streams delineated by means of curvature-based method (Figure 2(b)). The values of cell-to-stream length, *L(x, y)*, were computed using the TauDEM software (http://hydrology.neng.usu.edu/taudem/). The covariance function was used to compute the autocorrelation length of *L(x, y)*, which we have calculated to be about 100 cells or 3.7 km. The resultant map of drainage density is shown in Figure 4(a). Some noticeable circular features are artifacts of using a circular window to calculate ⟨*L*⟩. Overall, this map of *D* is much superior to the map based on watershed basins (Figure 3(b)) inasmuch as it matches much more closely the actual dissection as shown in Figure 2(b). A continuous raster format of this map facilitates correlation analysis with candidates for dissection control factors, which are mostly given in the raster form (except the geologic map).

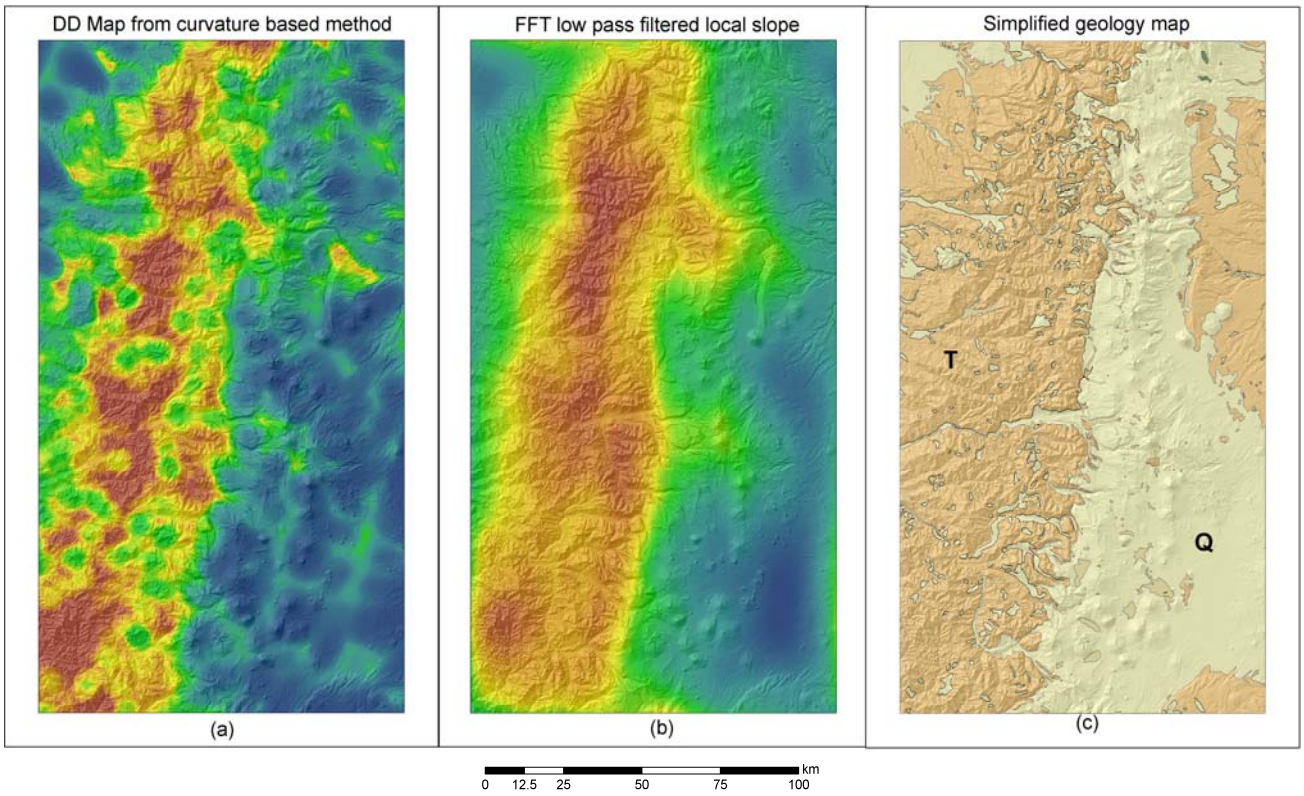

Fig. 4 (a) Drainage density map, the blue to orange color gradation indicates low to high values from a minimum of 0.012 km^{-1} to a maximum of 1.87 km^{-1}; (b) smoothed local slope derived from FFT low pass filter at 28 km scale, the blue to orange color gradation indicates low to high values from a minimum of 1.04˚ to a maximum of 19.65˚; (c) simplified geologic map. The original units were merged into two major units by age. T = Tertiary, Q = Quaternary. The shaded relief is shown in the background in all three maps.

3.3 Regional pattern of dissection – candidate controlling factors

The most striking feature of the study area is the sharp contrast in degree of dissection between its western and eastern parts (see Figure 2(b) and Figure 4(a)). We consider a number of terrain (local slope, regional slope), geologic (rock age), and environmental (annual mean precipitation) factors that may be responsible for this contrast. We use the continuous map of drainage density as a representation of the terrain dissection pattern (Figure 4(a)), and look for visual and formal correlations between the pattern of drainage density and patterns of candidate control factors.

3.3.1 Local slope

The local slope is defined as the largest slope between a given cell and its eight neighboring cells. This is a slope measured at the smallest possible baseline. We have calculated a raster of local slopes (not depicted here); the spatial correlation coefficient [25] between that raster and the map of *D* is 0.62. In addition to considering a local slope we have also consider a regional trend of local slope by applying the low pass filter (implemented using the Fast Fourier Transform (FFT)) to the raster of local slopes. To understand the result of such transformation, it is convenient to envision the raster of local slopes as an image. The low pass filter blurs an image by removing short scale variability from it. The result, in our case, is a raster that represents only long scale variability of the local slope. Figure 4(b) shows the results of applying the low pass filter with a cutoff of 28 km to the raster of local slopes. Comparing the low pass raster to the 3-D landscape (Figure 1) reveals that, on long scale, high local slopes are present in the western part of the study area, where the average relief and terrain roughness are high, and the low local slopes are present in the eastern part of the study area, where the average relief and terrain roughness are low. Thus, the low pass raster may constitute a proxy for terrain roughness. There is a striking similarity in spatial distribution between the maps of *D* (Figure 4(a)) and local slope truncated to long scale component or roughness (Figure 4(b)). The spatial correlation coefficient between the two grids is 0.85 confirming a high degree of correspondence.

Table 1 Correlation coefficient between drainage density and other factors

local slope		regional slope at different baseline					precipitation
original	FFT smoothed	31 km	21 km	11 km	5 km	1 km	
0.62	0.85	-0.093	-0.032	0.19	0.35	0.4	0.55

3.3.2 Regional slope

The regional slope is defined as the slope of terrain measured over a regional baseline. We have calculated the regional slope by fitting a plane to the 3-D points on the surface *(x,y,z),* where *(x,y)* are raster coordinates located within a square having dimensions equal to a given baseline and centered on a focus cell. The angle between the fitted plane and the horizontal plane is the regional slope assigned to a focus cell. The raster of regional slopes can be understood as the raster of slopes in a surface that was stripped of all of its details on a given scale. Figure 5(b) shows the regional slope calculated for our study area using the baseline of 31 km. Comparing regional slope to the 3-D landscape (Figure 1) clarifies the notion of regional slope. There is no significant correlation between maps of *D* (Figure 5(a)) and 31 km baseline regional slope (Figure 5(b)); the correlation coefficient is -0.093. In Table 1 we list the values of correlation coefficients between the maps of *D* and regional slope calculated for various baselines. As the baseline decreases, the correlation coefficient increases, up to the value of 0.4 for the 1 km baseline. This suggests that drainage density in our study area is not controlled by regional slope. There is a correlation between a drainage density and the slope calculated on much smaller length scale, but the cause and effect relation is not clear and will be discussed below.

3.3.3 Mean annual precipitation

The map of mean annual precipitation is shown in Figure 5(c). There is a sharp contrast in precipitation between the far eastern portion of the study area and the rest of it due to an orographic effect on rainfall, but the location of the precipitation contrast does not coincide with the location of the drainage density contrast, and the correlation coefficient is only 0.55. Thus, precipitation is not likely to be an important factor responsible for an observed variability in landscape dissection.

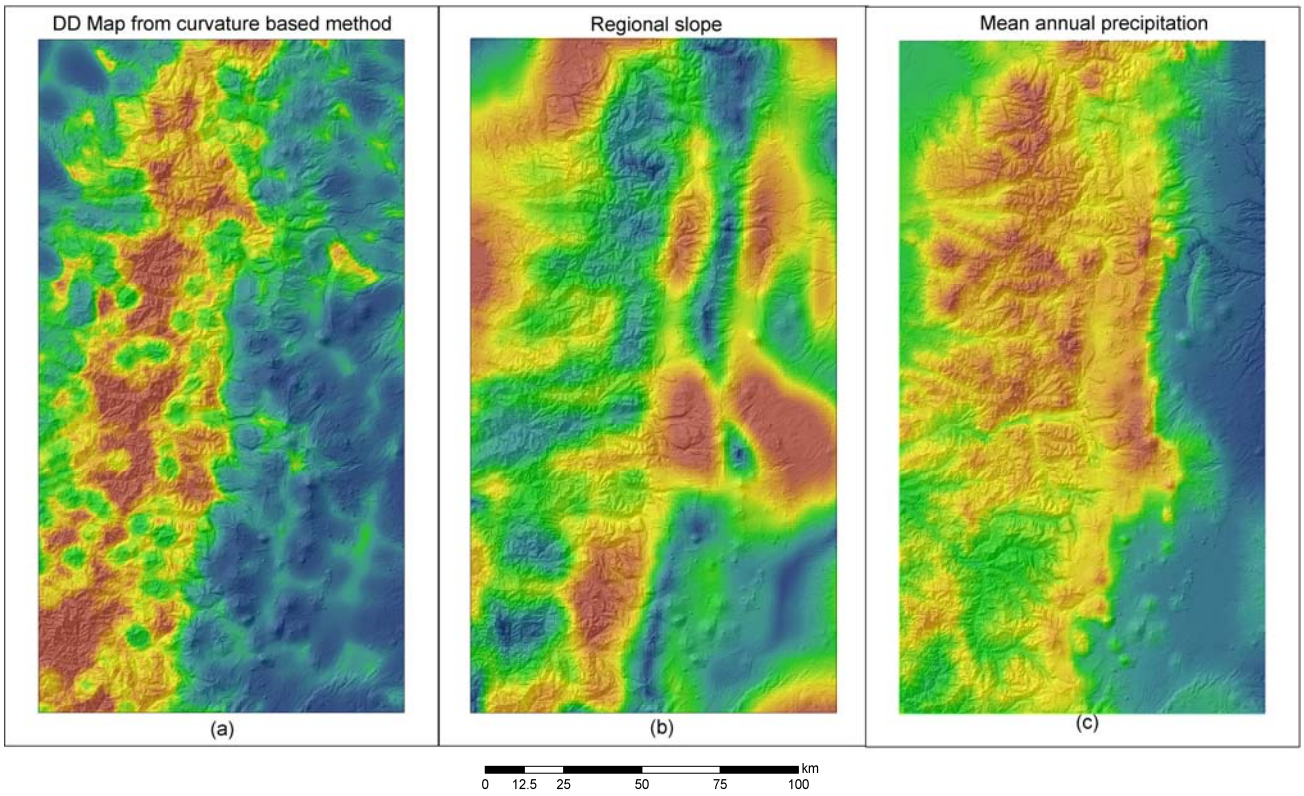

Fig. 5 (a) Drainage density map, min = 0.012 km^{-1}, max = 1.87 km^{-1}, same as Figure 4(a), repeated here for easy comparison; (b) regional slope at 31km baseline, min = 0.002˚, max = 2.623˚; (c) Mean annual precipitation, min = 245.45 mm, max = 3149.36 mm. The shaded relief is shown in the background in all three maps.

3.3.4 Geologic age

Lastly, we consider the site's geology as a factor responsible for a pattern of dissection in the study area. Figure 4(c) shows a simplified geologic map of the study area obtained by merging different geological units into two major groups on the basis of age: Quaternary (Q) and Tertiary (T). As explained in Section 2, this partition corresponds to a division into Western Cascades and High Cascades. The sharp geographical contrast between the Q and T zones corresponds closely to the location of the drainage density contrast. High dissection is restricted mostly to Western Cascades (T), and the low dissection is restricted mostly to High Cascades (Q). We calculated the zonal statistics of drainage density within the zones of Q and T. The result is summarized in Table 2. Statistical *t* test shows that the mean drainage density of Quaternary is significantly lower than that of the Tertiary (the difference is highly statistically significant with *t*=-*2974.2*). Thus, the geology seems to be the major factor controlling the pattern of drainage density in our study area, not only because of high spatial correspondence between the geologic and drainage density patterns, but also because geologic control makes physical sense. The Western Cascades are older and the alteration of minerals (especially the formation of clays) tends to close pore space, reducing permeability and thus promoting surface runoff resulting in more incision, steeper local slope, and higher drainage density [26, 27, 23]. The High Cascades are young and much more permeable, thus promoting infiltration of water reducing the surface runoff and resulting in less incision.

Table 2. Zonal statistics of drainage density within the zones of Q and T

Age	# of cells	Minimum	Maximum	Range	StdDev.	Mean
Q	8557244	0.01	1.64	1.63	0.23	0.27
T	9437284	0.03	1.87	1.84	0.37	0.71

4. CONCLUSION

In this paper we have demonstrated that high-resolution maps of drainage density can be automatically generated on regional scale from remotely sensed elevation data. The generation process relies on two crucial steps: reliable delineation of streams, and the at-point assignment of drainage density values to each cell in the raster. The first step cannot be executed using broadly available software packages, as it requires a delineation algorithm that does not make any assumptions about channelization mechanism. However, the curvature-based algorithm used in our calculation is available from the authors upon request. The second step (originally proposed by Tucker et al. [5]) breaks with the traditional method of calculating drainage density in favor of statistical calculation that yields high-resolution, continuous map of *D*. Why to map drainage density on regional scale? Because such mapping offers an automatic, and thus affordable, means of surveying large regions for variability in either geology, environment, or other quantity of interest, which by themselves are difficult to sense remotely. Spatial variability present in such quantities manifests themselves through variability in drainage density, which is detected by our proposed method.

We have demonstrated this concept on the study area located in Cascade Range, Oregon, USA. The generated map of drainage density reveals a sharp contrast indicating abrupt change in some underlying quantity. We consider local and regional slope, mean annual precipitation, and geology as spatial variables that may happen to change abruptly within the study area and cause the observed pattern of *D*. The regional slope has been eliminated from the list of possible factors because its pattern of variability is not correlated with the pattern of *D*. However, the remaining three factors are all correlated to significant degree with the map of *D*. Of the three, the mean annual precipitation is the least correlated with *D* and we believe that the partial alignment of its pattern with the pattern of *D* is a coincidence rooted in Oregon geography. The local slope is highly correlated with *D*, however we believe that it is not a cause of the observed contrast in drainage density, but rather its effect. This leaves geology as the most likely cause of the observed pattern of *D*. Indeed the geology correlates highly with the map of *D*, and its description within the study area further indicates its dominant role in controlling the pattern of drainage density.

In the case of our study area all possible controlling factors are known a priori. However, we envision a scenario, where spatial variation in geology or other factors, are not known, and our method may be applied to reveal the existence of such variations. Such application may be relevant to parts of the world less studied than the Cascade Range, or to the exploration of other planets.

Acknowledgements.

TFS acknowledges support by NASA under grant NNG05GM31G. A portion of this research was conducted at the Lunar and Planetary Institute, which is operated by the USRA under contract CAN-NCC5-679 with NASA. This is LPI Contribution No. ….

REFERENCES

1. Montgomery, D.R. and W.E. Dietrich, Source areas, drainage density, and channel initiation. *Water Resources Research*, 25(8): 1907-1918 (1989).
2. Tarboton, D.G., R.L. Bras, and I. Rodriguez-Iturbe, A physical basis for drainage density. *Geomorphology*, 5(1-2): 59-76 (1992).
3. Oguchi, T., Drainage Density and Relative Relief in Humid Steep Mountains with Frequent Slope Failure. *Earth surface processes and landforms*, 22(2): 107 (1997).
4. Tucker, G.E. and R.L. Bras, Hillslope processes, drainage density, and landscape morphology. *Water Resources Research*, 34(10): 2751-2764 (1998).
5. Tucker, G.E., et al., Statistical analysis of drainage density from digital terrain data. *Geomorphology*, 36: 187–202 (2001).

6. Rodriguez-Iturbe, I., A. Rinaldo, and D.R. Mongomery, Fractal River Basins: Chance and Self-Organization. *Nature*, 396(6711): 1 (1998).
7. Horton, R.E., Drainage basin characteristics. *American Geophysical Union Transactions*, 13: 348-352 (1932).
8. Chorley, G., Climate and morphometry. *Journal of Geology*, 65: 628-638 (1957).
9. Gregory, K.J. and V. Gardiner, Drainage density and climate. *Zeitschrift fur Geomorphologie*, 19: 287-298 (1975).
10. Melton, M.A., Coreelation structure of morphometric properties of drainage syustems and their controlling agents. *Journal of Geology*, 66: 442-460 (1958).
11. Wilson, L., Drainage density, length ratios, and lithology in a glaciated area of southern Connecticut. *Geological Society of America Bulletin*, 82: 2955-2956 (1971).
12. Kelson, K.I. and S.G. Wells, Geologic influences on fluvial hydrology and bedload transport in small mountainous watersheds, northern New Mexico, USA. *Earth surface processes and landforms*, 14: 671-690 (1989).
13. Schumm, S.A., Evolution of drainage systems and slopes in badlands at Perth Amboy, New Jersey. *Geological Society of America Bulletin*, 67: 597-646 (1956).
14. Morisawa, M., Accuracy of determination of stream length from topographic maps. *Transactions of the American Geophysical Union*, 38: 86-88 (1957).
15. O'Callaghan, J.F. and D.M. Mark, The extraction of drainage networks from digital elevation data. *Computer Vision, Graphics and Image Processing*, 28: 323-344 (1984).
16. Tarboton, D.G., R.L. Bras, and I. Rodriguez-Iturbe, On the Extraction of Channel Networks from Digital Elevation Data. *Hydrological processes*, 5: 81-100 (1991).
17. Montgomery, D.R. and W.E. Dietrich, Channel Initiation and the Problem of Landscape Scale. *Science*, 255(5046): 826-829 (1992).
18. Tarboton, D.G. and D.P. Ames. *Advances in the mapping of flow networks from digital elevation data*. in *World Water and Environmental Resources Congress*. 2001. Orlando, Florida: ASCE.
19. Peuker, T.K. and D.H. Douglas, Detection of surface-specific points by local parallel processing of discrete terrain elevation data. *Computer Graphics and Image Processing*, 4: 375-387. (1975).
20. Molloy, I. and T.F. Stepinski, Automatic Mapping of Valley Networks on Mars. *Computers and Geosciences*: in press (2007).
21. Walker, G.W. and N.S. MacLeod, *Geologic map of Oregon, special geologic map, 2 sheets*. 1991, U.S. Geologic Survey: Reston, VA.
22. Sherrod, D.R. and J.G. Smith, *Geologic map of upper Eocene to Holocene volcanic and related rocks of the Cascade Range, Oregon*, in *U.S. Geological Survey Investigation Series*. 2000. p. 17 pp.
23. Tague, C. and G.E. Grant, A geological framework for interpreting the low-flow regimes of Cascade streams, Willamette River basin, Oregon. *Water Resources Research*, 40, no. 4(4)(2004).
24. Luo, W. and T.F. Stepinski, Planets - L18202 - Topographically derived maps of valley networks and drainage density in the Mare Tyrrhenum quadrangle on Mars (DOI 10 1029/2006GL027346). *Geophysical research letters*, 33(18): n. (2006).
25. Goodchild, M.F., *Spatial autocorrelation*. Catmog. Vol. 47. Norwich.: Geo Books 1986.
26. Ambers, R.K.R., Relationships between clay mineralogy, hydrothermal metamorphism, and topography in a Western Cascades watershed, Oregon, USA. *Geomorphology*, 38(1): 16 (2001).
27. Perron, J.T., M. Manga, and M.P. Lamb. *Permeability, recharge, and runoff generation on Mars*. in *Workshop on Martian Valley Networks*. 2004. Hawaii.